Pamela L. Dickrell

N. Argibay

Department of Mechanical and Aerospace Engineering,
University of Florida,
Gainesville, FL 32611

Osman L. Eryilmaz

Ali Erdemir

Energy Technology Division,
Argonne National Laboratory,
Argonne, IL 60439

W. Gregory Sawyer

Department of Mechanical and Aerospace Engineering,
University of Florida,
Gainesville, FL 32611

Temperature and Water Vapor Pressure Effects on the Friction Coefficient of Hydrogenated Diamondlike Carbon Films

Microtribological measurements of a hydrogenated diamondlike carbon film in controlled gaseous environments show that water vapor plays a significant role in the friction coefficient. These experiments reveal an initial high friction transient behavior that does not reoccur even after extended periods of exposure to low partial pressures of H_2O and O_2. Experiments varying both water vapor pressure and sample temperature show trends of a decreasing friction coefficient as a function of both the decreasing water vapor pressure and the increasing substrate temperature. Theses trends are examined with regard to first order gas-surface interactions. Model fits give activation energies on the order of 40 kJ/mol, which is consistent with water vapor desorption.
[DOI: 10.1115/1.3139047]

Keywords: gas-surface interactions, humidity, DLC, environment, ultra low friction, adsorption

1 Introduction

Diamondlike carbon (DLC) films are of interest in tribology as solid lubricant coatings for sliding interfaces. DLC films can be made by plasma enhanced chemical vapor deposition (PECVD) or physical vapor deposition techniques. A range of mechanical properties and chemical compositions of DLC films can be achieved. The specific type of DLC coating examined in this work is a highly-hydrogenated form of DLC developed at Argonne National Laboratory. When self-mated and operated in inert atmospheres, this film can sustain friction coefficients as low as $\mu = 0.003$, which is in the superlow friction regime of $\mu < 0.01$; this coating was thus termed "near-frictionless carbon" (NFC) [1]. In this superlow friction regime, the wear rates are also extraordinarily low, $K < 3 \times 10^{-10}$ mm^3/N m. The specific NFC films investigated in this study use 25% CH_4 and 75% H_2 for chamber flow ratios during coating deposition [2]. The resulting film has atomic percentages of approximately 60% carbon and 40% hydrogen and is between 1 μm and 1.5 μm thick [3]. Indentation tests have reported a hardness of 7.7 GPa and an elastic modulus of 47 GPa [1]. Additionally, Raman spectroscopy has indicated that these NFC films have approximately 60% sp^3-bonding in their composition, with the majority of the sp^3 bonds being hydrogen terminated [4].

It has been proposed that the superlow friction behavior of self-mated NFC films is due to the inertness of the hydrogen terminated interface, which is thought to exert very little adhesive and frictional forces when sliding against itself [2]. The films used in this study have high hydrogen content, and it has been theorized that free hydrogen in these films can terminate carbon bonds at the surface [3]. Hydrogen may passivate dangling surface bonds of carbon atoms and reduce the friction coefficient; when the hydrogen is removed the friction coefficient increases [2]. It has also been observed that in a self-mated NFC pair, the superlow friction found in an inert environment [3] increases when active gaseous species are added [5]. Hypotheses are that various gases can disrupt the hydrogen termination of the NFC pair and lead to an increase in friction coefficient. NFC films only realize low coefficients of friction and wear rates in inert, dry, or vacuum environments [1–3,5,6]. In contrast, hydrogen-free diamondlike carbon films show their lowest friction coefficients in humid air [7], further suggesting the importance of surface hydrogen on friction.

It has been long theorized that gas adsorption is the cause for variation in the friction coefficient and wear rate of the films [3,5,6]. Heimberg et al. [6] demonstrated that the velocity dependence of the friction coefficients of NFC films could be explained by exposure time. In addition, Heimberg et al. modeled the transient frictional behavior using an Elovich model for adsorption and a "wiping" model for material removal [6]. Modeling of the transient and steady-state behavior was developed by combining the material removal models of Blanchet and Sawyer [8] with the Langmuir adsorption [9]. Such models compared favorably to the experimental results of Heimberg et al. [10]. The positional dependence of friction coefficient along the reciprocating track was compared with an extended version of this model that included variable exposure times along the reciprocating track length [11].

This includes the effects of temperature. Previous experimental and theoretical efforts have implicated water vapor as the driver in the frictional behavior of these films. It can be readily hypothesized that increased sample temperature should decrease the coverage of water on the surfaces and thus decrease the friction coefficient.

2 Experimental Apparatus

A low contact pressure tribometer enclosed in an environmental chamber was used in this study for all friction coefficient measurements (a schematic of the contact region of this tribometer is shown in Fig. 1). Dry argon (manufacturer reported purity of better than 5 ppm water and oxygen) was used as the background gas. During testing a positive chamber pressure ($\sim$3 KPa) was maintained and measured, and an oxygen detector continuously sampled the environment to ensure that the partial pressure of oxygen was less than 20 ppm. Elevated surface temperatures were achieved by encapsulating a resistive heater under the counterface

Contributed by the Tribology Division of ASME for publication in the JOURNAL OF TRIBOLOGY. Manuscript received April 27, 2007; final manuscript received April 24, 2009; published online May 27, 2009. Assoc. Editor: Mitjan Kalin.

Report Documentation Page

Form Approved
OMB No. 0704-0188

1. REPORT DATE	2. REPORT TYPE	3. DATES COVERED
JUL 2009		**00-00-2009 to 00-00-2009**

4. TITLE AND SUBTITLE	5a. CONTRACT NUMBER
Temperature and Water Vapor Pressure Effects on the Friction Coefficient of Hydrogenated Diamondlike Carbon Films	5b. GRANT NUMBER
	5c. PROGRAM ELEMENT NUMBER
6. AUTHOR(S)	5d. PROJECT NUMBER
	5e. TASK NUMBER
	5f. WORK UNIT NUMBER
7. PERFORMING ORGANIZATION NAME(S) AND ADDRESS(ES) **University of Florida,Department of Mechanical and Aerospace Engineering,Gainesville,FL,32611**	8. PERFORMING ORGANIZATION REPORT NUMBER
9. SPONSORING/MONITORING AGENCY NAME(S) AND ADDRESS(ES)	10. SPONSOR/MONITOR'S ACRONYM(S)
	11. SPONSOR/MONITOR'S REPORT NUMBER(S)

12. DISTRIBUTION/AVAILABILITY STATEMENT
Approved for public release; distribution unlimited

13. SUPPLEMENTARY NOTES

14. ABSTRACT

15. SUBJECT TERMS

16. SECURITY CLASSIFICATION OF:			17. LIMITATION OF ABSTRACT	18. NUMBER OF PAGES	19a. NAME OF RESPONSIBLE PERSON
a. REPORT **unclassified**	b. ABSTRACT **unclassified**	c. THIS PAGE **unclassified**	**Same as Report (SAR)**	**5**	

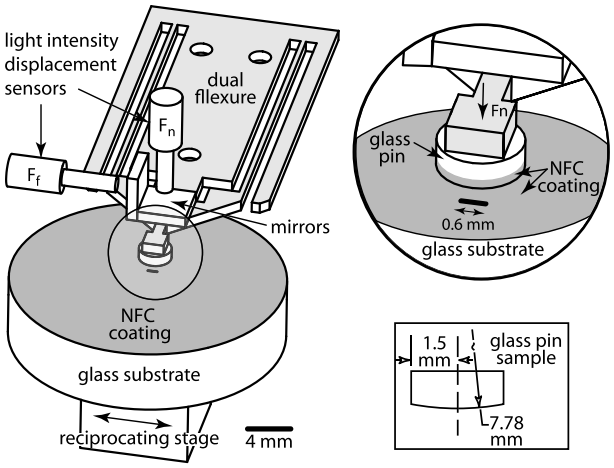

Fig. 1 Schematic of the contact region of the low contact pressure tribometer

and was measured using a thermocouple that was adhered onto the sample surface. The pin and counterface samples were borosilicate glass that were coated with NFC; the pins had a 7.78 mm radius of curvature. The initial surface roughnesses were approximately $R_a=3.2$ nm, as measured by a scanning white-light interferometer, and the film thicknesses were on the order of a micrometer.

3 Results and Discussion

An initial run-in experiment in the argon environment was performed on the as-deposited NFC coatings. The applied normal load (F_n) was 100 mN, the track length (L) was 0.6 mm, and the sliding speed (V) was 18 mm/s. Under the 100 mN load, the Hertzian track width was approximately 50 μm. As shown in Fig. 2, it took over 2000 cycles (N) of high friction ($\mu \sim 0.5$) sliding before running-in to a low friction coefficient condition. The energy (U) dissipated during the run-in period can be estimated by $U=2\mu F_n LN$, and approximately 120 mJ of energy was dissipated during this regime. Previously, neutron reflectivity demonstrated that the as-deposited NFC films are composed of two layers with an approximately 30 Å thick higher density surface layer over the bulk [12]. In this argon environment the wear of the films was very low, and post-test analysis of the wear tracks and wear scars revealed that the wear was below our ability to report quantitative wear rates using scanning white-light interferometry.

A series of experiments were run on the same wear track without breaking the dry argon environment in order to assess whether or not a similar high friction layer could reform in the testing

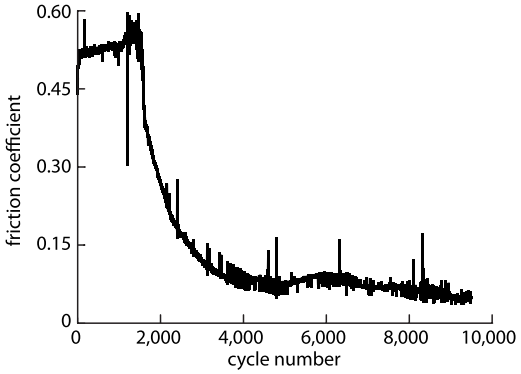

Fig. 2 Initial run-in of two as-deposited self-mated NFC samples in a dry argon environment

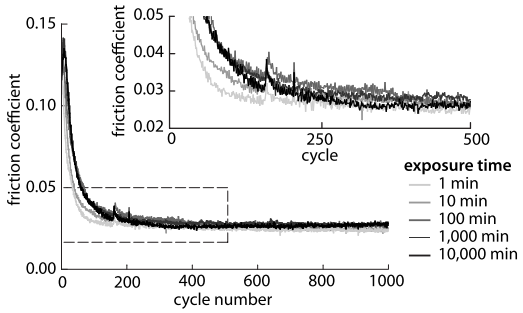

Fig. 3 Friction coefficients for repeated sliding at the same location after separating the surface for specified periods of time in a dry argon environment

environment. The contact was separated randomly by orders of magnitude from 1 min to 10,000 min. After this aging of the samples, the transient friction behavior of the films was again examined using a "standard" test that consisted of 1000 cycles at 5 mm/s, under 3 mN of load, over a 0.6 mm track. Plots of the friction coefficient trends after the periods of dwell for each standard test are shown in Fig. 3. It was clear that regardless of dwell time the high friction run-in behavior did not return. For these experiments the initial friction coefficient value began at approximately $\mu=0.13$, which is close to the highest steady-state friction coefficient for a self-mated NFC pair seen by Heimberg et al. [6].

In another experiment, water vapor was added to the chamber without increasing the oxygen partial pressure above 20 ppm. An experiment was run where the environment started as dry argon, the friction coefficient was allowed to run-in to a low value, and then the amount of water vapor was ramped up and back down to see how the friction coefficient responded to these changes in relative humidity (RH) (this is plotted in Fig. 4). This experiment clearly demonstrated that water vapor is a species that adversely affects the friction coefficient. It is also clear that even at $\sim$32% RH the high initial friction coefficient ($\mu \sim 0.5$) seen in Fig. 2 was not observed, and the highest friction coefficient is similar to the starting friction coefficient values found during the exposure experiments shown in Fig. 3.

A series of experiments varying both the chamber water vapor pressure and the counterface surface temperature was designed and executed with the hope to correlate trends in friction coefficient to water adsorption and desorption kinetics. A single self-mated NFC coated pin and counterface sample were used for the entire matrix of experiments, and the experiments were all performed in the same wear track. The experimental matrix for this series consisted of four individual experiments. During each ex-

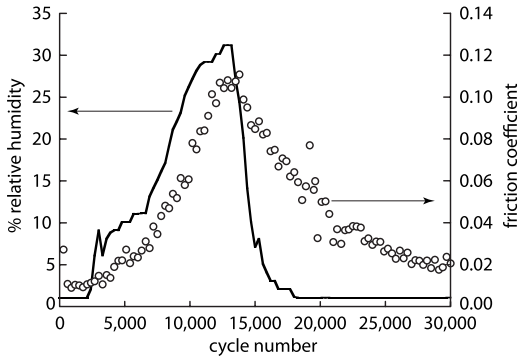

Fig. 4 Friction coefficients over a single experiment ramping the water vapor concentration while holding the oxygen partial pressure below 20 ppm. Under a contact load of 200 mN and a sliding speed of 4 mm/s.

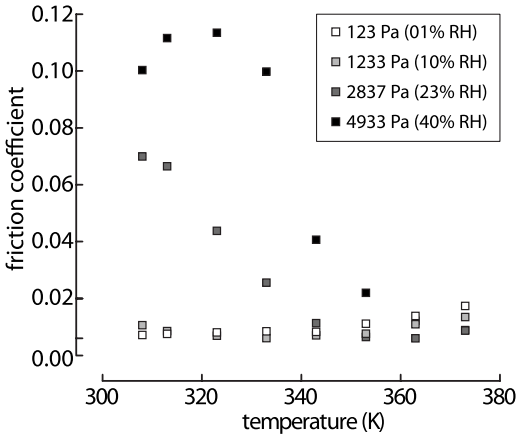

Fig. 5 Experimental results of friction coefficient (μ) as a function of counterface surface temperature and water vapor pressure

periment the chamber water vapor pressure was held at a distinct prescribed value, ranging from 123 Pa to 4933 Pa. Each experiment consisted of 32,000 cycles of sliding under a 100 mN normal load, at a sliding speed of 18 mm/s, over a 0.6 mm track length. The counterface surface temperature was held for 4000 cycles of sliding at eight distinct temperatures ranging from 308 K to 373 K. The friction coefficients reported are the average values from cycles 3500–4000 at each temperature step, and are plotted collectively in Fig. 5. In the experiments with vapor pressures below 1233 Pa, low friction was maintained over the entire range of surface temperatures. However, when the water vapor pressure was 2837 Pa and 4933 Pa, a low friction coefficient was achieved only at temperatures above 340 K and 360 K, respectively.

4 Modeling/Discussion

Comparisons of friction coefficient to a fractional coverage (θ) of a contaminant on the exposed surface of the counterface are common in vapor and gas phase lubrication studies. Here the coverage on the pin sample, which is always in contact, was assumed to be zero. In order to estimate an equivalent coverage for a given condition, the friction coefficient was assumed to follow a linear rules of mixture [10,11], as shown in Eq. (1)

$$\theta = \frac{(\mu - \mu_0)}{(\mu_1 - \mu_0)} \tag{1}$$

In Eq. (1), μ_0 is the friction coefficient of a clean surface, and μ_1 is the friction coefficient of a fully saturated surface. Friction coefficient values for the nascent (clean) and fully covered surfaces from previous modeling efforts were reported to be $\mu_0 = 0.006$ and $\mu_1 = 0.12$, respectively [10,11].

The surface coverage changes in water vapor pressure (P) and counterface temperature (T) can be examined using Langmuir's model of surface adsorption and desorption [13]; we assume that the sticking coefficient is unity. Table 1 outlines the modeling parameters. The Langmuir model gives the change in surface coverage as a function of time assuming an adsorption rate ($K_a P$) over the nascent portion of the surface ($1-\theta$) minus the desorption rate (K_d), as given by Eq. (2)

$$\frac{d\theta}{dt} = K_a P(1 - \theta) - K_d \theta \tag{2}$$

Assuming an initial coverage of θ_0, Eq. (2) can be solved to give the coverage as a function of the rates of adsorption, desorption, and time (t); this is given in Eq. (3). At steady-state this expression is simplified to Eq. (4)

Table 1 Gas-surface modeling nomenclature

Symbol	Units	Definition
E_a	J/mol	Energy to dissociate from surface
I	No./cm^2 s	Molecular impingement rate
k	J/K	Boltzmann constant
K_a	1/Pa s	Adsorption rate coefficient
K_d	1/s	Desorption rate
m	kg	Molecular mass
n_0	sites/m^2	Site density
P	Pa	Pressure
Subscript SS	n/a	Steady state
t	s	Time
T	K	Temperature
τ_a	s	Average stay time
τ_0	s	Time between attempts
θ	*	Covered fraction
$1-\theta$	*	Nascent fraction

$$\theta = \frac{K_a P}{K_a P + K_d} + \left(\theta_0 - \frac{K_a P}{K_a P + K_d}\right) e^{-(K_a P + K_d)t} \tag{3}$$

$$\theta_{SS} = \frac{K_a P}{K_a P + K_d} \tag{4}$$

The expression for the adsorption rate coefficient (K_a) is given by Eq. (5) [13,14]. In this expression, the adsorption rate coefficient is a function of the molecular impingement rate (I), the surface site density (n_0), and the pressure (P). The adsorption rate coefficient can also be expressed as a function of the site density (n_0), molecular mass (m), the Boltzmann constant (k), and the temperature (T)

$$K_a = \frac{I}{n_0 P} = \frac{1}{n_0 (2\pi m k T)^{1/2}} \tag{5}$$

Here all parameters are estimated. The site density (n_0) is estimated as 1.3×10^{19} sites/m^2 and 2.99×10^{-26} kg is used as the molecular mass of water. The Boltzmann constant is defined as 1.3807×10^{-23} J/K. The appropriate temperature is assumed to be the chamber temperature, which was held constant at 303 K. This gives $K_a = 2838$ Pa^{-1} s^{-1}.

The desorption rate is given in Eq. (6) [13,14], and is defined as the inverse of the average staying time (τ_a) of a molecule on the surface. The desorption rate is a function of the time between molecular escape attempts (τ_0), the activation energy (E_a), the Boltzmann constant, and the temperature.

$$K_d = \frac{1}{\tau_a} = \frac{1}{\tau_0} e^{(E_a/kT)} \tag{6}$$

The important temperature for the desorption process is the counterface surface temperature, which was controlled during the experiments.

Figure 6(a) shows the fit of Eq. (4) to the data plotted in Fig. 5. A least-squares regression optimization returns attempt times of $\tau_0 = 2.5 \times 10^{-15}$ s and an activation energy of $E_a = 46.5$ kJ/mol. The inverse of the crystal lattice vibrational frequency may be used to estimate of the time between molecular surface escape attempts [13], and gives values on the order of $\tau_0 = 1 \times 10^{-13}$ s. It turns out that the fits are not particularly sensitive to attempt times of this order of magnitude. If the activation energy is treated as a free parameter, the fits improve slightly (Fig. 6(b)) and give values of activation energy between 40–50 kJ/mol. These activation energies are comparable to other investigations of water desorption that report activation energies on the order of 40 kJ/mol [15,16].

While water vapor is a clearly shown to be a contributing factor to the tribological performance of these self-mated highly-

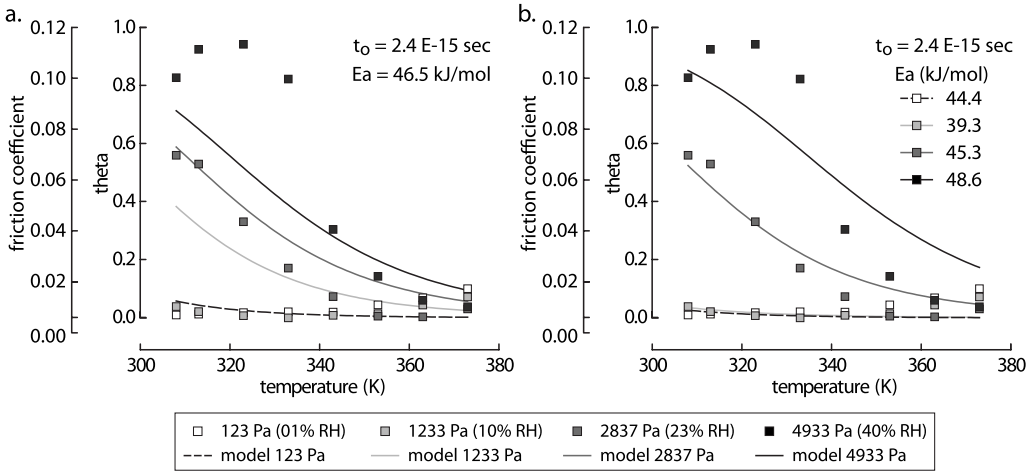

Fig. 6 Model fit of Eq. (5) to experimental data with (*a*) a universally fit value for τ_0 and E_a and (*b*) a universally fit value of τ_0 and a variable fit of E_a

hydrogenated diamondlike carbon films, this adsorption model has a major deficiency in time scale. The transient behaviors predicted by this model have time constants on the order of nanoseconds not minutes (see Figs. 3 and 4). This may be partially explained by studies of water molecules adsorbing and desorbing on a hydrogen terminated diamond surface using X-ray photoelectron spectroscopy (XPS) and high resolution electron energy loss spectroscopy (HREELS) [17]. This XPS and HREELS study suggested that physisorbed water is the dominant mechanism on hydrogen terminated diamond surfaces. Other hypotheses involve the formation of water layers on the surfaces, and if data are plotted as friction coefficient versus the surface relative humidity (Fig. 7), there is a trend of decreasing friction coefficient versus relative humidity, but the data do not collapse onto a single curve. Based on these experiments, superlow friction appears to be limited to local relative humidities below 1–2%. The details of water's interactions with carbon films and its impacts on friction coefficient remain an open research question.

5 Conclusions

Low friction coefficients were achieved under microtribological (low contact pressure) sliding contacts of self-mated NFC.

An initial high friction film was shown to take over 2000 repeated passes prior to providing low friction.

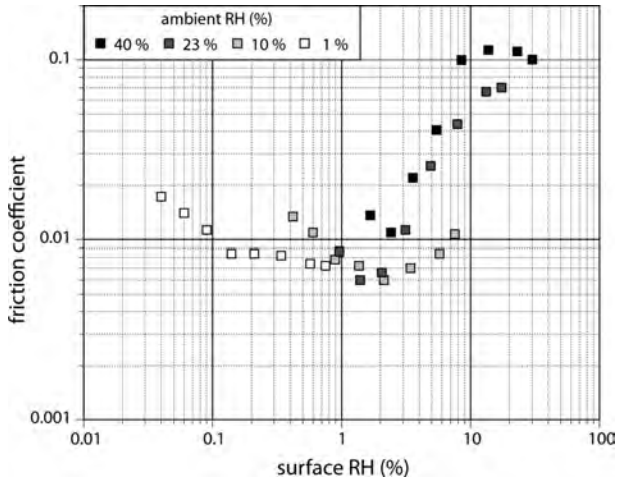

Fig. 7 Plot of the friction coefficient versus the relative humidity at the heated sample surface

Experiments varying the exposure time between contacts from 1 min to 10,000 min showed nearly identical transient behavior in friction coefficient.

Water vapor was shown to cause a high friction coefficient response, and though recoverable, the time constants were on the order of thousands of seconds.

Temperature and water vapor experiments showed trends of decreasing friction coefficient with combinations of decreasing water vapor pressure and increasing substrate temperature.

Acknowledgment

This material is based on an AFOSR-MURI Grant No. FA9550-04-1-0367.

References

[1] Erdemir, A., Eryilmaz, O. L., Nilufer, I. B., and Fenske, G. R., 2000, "Synthesis of Superlow-Friction Carbon Films From Highly Hydrogenated Methane Plasmas," Surf. Coat. Technol., **133-134**, pp. 448–454.

[2] Erdemir, A., Eryilmaz, O. L., Nilufer, I. B., and Fenske, G. R., 2000, "Effect of Source Gas Chemistry on Tribological Performance of Diamond-Like Carbon Films," Diamond Relat. Mater., **9**, pp. 632–637.

[3] Erdemir, A., 2001, "The Role of Hydrogen in Tribological Properties of Diamond-Like Carbon Films," Surf. Coat. Technol., **146-147**, pp. 292–297.

[4] Casiraghi, C., Piazza, F., Ferrari, A. C., Grambole, D., and Robertson, J., 2005, "Bonding in Hydrogenated Diamond-Like Carbon by Raman Spectroscopy," Diamond Relat. Mater., **14**, pp. 1098–1102.

[5] Andersson, J., Erck, R. A., and Erdemir, A., 2003, "Frictional Behavior of Diamondlike Carbon Films in Vacuum and Under Varying Water Vapor Pressure," Surf. Coat. Technol., **163–164**, pp. 535–540.

[6] Heimberg, J. A., Wahl, K. J., Singer, I. L., and Erdemir, A., 2001, "Superlow Friction Behavior of Diamond-Like Carbon Coatings: Time and Speed Effects," Appl. Phys. Lett., **78**, pp. 2449–2451.

[7] Andersson, J., Erck, R. A., and Erdemir, A., 2003, "Friction of Diamond-Like Carbon Films in Different Atmospheres," Wear, **254**, pp. 1070–1075.

[8] Blanchet, T. A., and Sawyer, W. G., 2001, "Differential Application of Wear Models to Fractional Thin Films," Wear, **251**, pp. 1003–1008.

[9] Langmuir, I., 1916, "The Constitution and Fundamental Properties of Solids and Liquids," J. Am. Chem. Soc., **38**, pp. 2221–2295.

[10] Dickrell, P. L., Sawyer, W. G., and Erdemir, A., 2004, "Fractional Coverage Model for the Adsorption and Removal of Gas Species and Application to Superlow Friction Diamond-Like Carbon," ASME J. Tribol., **126**, pp. 615–619.

[11] Dickrell, P. L., Sawyer, W. G., Heimberg, J. A., Singer, I. L., Wahl, K. J., and Erdemir, A., 2005, "A Gas-Surface Interaction Model for Spatial and Time-Dependent Friction Coefficient in Reciprocating Contacts: Applications to Near-Frictionless Carbon," ASME J. Tribol., **127**, pp. 82–88.

[12] Johnson, J. A., Woodford, J. B., Erdemir, A., and Fenske, G. R., 2003, "Near-Surface Characterization of Amorphous Carbon Films by Neutron Reflectivity," Appl. Phys. Lett., **83**, pp. 452–454.

[13] Hudson, J. B., 1998, *Surface Science: An Introduction*, Wiley, New York.

[14] Adamson, A. W., and Gast, A. P., 1997, *Physical Chemistry of Surfaces*, 6th ed., Wiley, New York.
[15] Biener, J., Lang, E., Lutterloh, C., and Kuppers, J., 2002, "Reactions of Gas-Phase H Atoms With Atomically and Molecularly Adsorbed Oxygen on Pt(111)," J. Chem. Phys., **116**, pp. 3063–3074.
[16] O'Hanlon, J. F., 2003, *A User's Guide to Vacuum Technology*, 3rd ed., Wiley, New York.
[17] Laikhtman, A., Lafosse, A., Le Coat, Y., Azria, R., and Hoffman, A., 2004, "Interaction of Water Vapor With Bare and Hydrogenated Diamond Films Surfaces," Surf. Sci., **551**, pp. 99–105.